Photochemical and Thermal Isomerization Processes of a Chiral Auxiliary Based Donor–Acceptor Substituted Chiroptical Molecular Switch: Convergent Synthesis, Improved Resolution and Switching Properties

Richard A. van Delden, Johannes H. Hurenkamp, and Ben L. Feringa*[a]

Abstract: A new type of chiroptical molecular switch is presented where irradiation employing different wavelengths of light induces a reversible helix inversion of a sterically overcrowded alkene bearing a second chiral entity in the form of a stereogenic center present in a pyrrolidine unit. The additional stereogenic center in the chiral auxiliary group has a distinct influence on the switching selectivity of this system and greatly facilitates the resolution of the different diastereoisomers, which is a considerable improvement compared with previously reported systems. In addition, the pyrrolidine stereogenic center causes small energetic differences between the various states of the switch system resulting in a small but significant directional preference in the helix inversion steps.

Keywords: chirality · isomerization · molecular devices · nanotechnology · photochromism

Introduction

In the different approaches towards true nanoscale molecular devices a variety of different functions have to be addressed at the molecular level.[1] This requires delicate supramolecular organization of different molecular components each capable of performing a certain function. A variety of molecular, mechanical type, components that might be part of the future toolbox of nanotechnology have been developed, including molecular counterparts of brakes,[2] gears,[3] turnstiles,[4] muscles,[5] and switches.[6]

Optical molecular switches play an important role in this endeavor.[6, 7] These photochromic systems might have potential use in applications such as optical data storage units, trigger elements, or as switching devices in optical data processing. In the pursuit of chiral optical (*chiroptical*) molecular switches, the unique properties associated with stereoisomers of chiral photochromic molecules and chiral supramolecular systems are exploited. Different approaches can be distinguished (Figure 1). The only approach resulting in switching between true enantiomers (Figure 1A) involves the use of circularly polarized light. The number of examples in this case is limited.[8] For most chiral photochromic systems known, switching, distant from the actual stereogenic center, results in a geometrical change in the molecules leading to a detectable change in for example chiroptical properties. Examples include among others chiral diarylethylenes,[9] azobenzenes,[10] spiropyrans,[11] and fulgides.[12] In those examples, the chirality of the systems itself does not change but the photoinduced geometrical change has an effect on the chiral properties (Figure 1B). Different wavelengths of light can be employed for switching between two states (0-X* $\rightleftharpoons$ 1-X*) but the properties of the two forms of such a bistable switching system, apart from the geometry-determined difference in chirality, are usually quite different due to the large difference in shape. This type of switches also includes a large variety of helically shaped polymer systems where a change in helicity can be affected by switching an achiral side-chain.[13] For these polymer systems the two forms of the bistable switching system can be considered pseudoenantiomeric. Our approach towards chiroptical molecular switches involves switching of pseudoenantiomeric forms (*P* and *M*′) of a sterically overcrowded alkene (Figure 1C).[14] Switching, employing different wavelengths of light, completely changes the chiral properties of the system. This has resulted in a number of selective molecular switches which were successfully applied as triggers for liquid crystal phase transitions.[15] The molecular switches have evolved towards true molecular motors in which consumption of photon energy results in controlled unidirectional rotation.[16] This motion could eventually enable a device to perform mechanical work.[17] In a new versatile second-generation design of our molecular motors the direction of rotation is solely governed by the interplay of a single stereogenic center with the intrinsic helical shape of the molecules.[18] The control of the direction of a full rotary motion in these molecular type motors is a

[a] Prof. Dr. B. L. Feringa, Dr. R. A. van Delden, J. H. Hurenkamp
Department of Organic and Molecular Inorganic Chemistry
Stratingh Institute, University of Groningen
Nijenborgh 4, 9747 AG Groningen (The Netherlands)
Fax: (+31)50-3634296
E-mail: feringa@chem.rug.nl

 DOI: 10.1002/chem.200204660

basic requirement for the construction of (supra)molecular machines.[1a]

Here, we report a newly developed pyrrolidine-based donor–acceptor switch where, in addition to the intrinsically chiral switch structure, a second chiral unit in the form of a stereogenic center in the pyrrolidine substituent is present. This system can be considered a hybrid between types B and C (Figure 1), where different wavelengths of light are used to switch between two helically shaped forms of a sterically overcrowded alkene bearing an additional chiral unit (Figure 1D). Some interesting features resulting from the interplay of the two chiral moieties (helix structure and asymmetric carbon center) present in the molecule can be anticipated. For example, where for previously reported chiroptical molecular switches chiral resolution was troublesome in all cases, we anticipated a positive influence of the chiral pyrrolidine moiety in the present case. With a focus on the influence of the chiral handle, the synthesis, resolution and physical properties and stereochemical pathways of this molecular switch are presented.

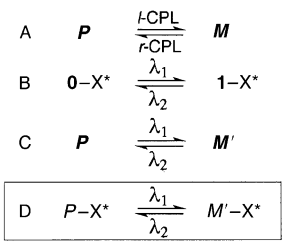

Figure 1. Schematic representation of different types of chiroptical molecular switches (X* = chiral auxiliary group).

Our binary molecular switching system is based on the *cis* and *trans* forms of a sterically overcrowded alkene with an intrinsic helical chirality. The two pseudoenantiomeric[19] forms of the molecular switch have an opposite helicity, that is negative helicity (*M*) in case of the *cis*-form and positive helicity (*P*) in case of the *trans*-form as illustrated for compound **1** (Scheme 1 top). Compound **1** is a typical example of our chiroptical molecular switches and one of the most successful switches developed so far.[20] For selective switching of **1**, the lower half of the molecules is functional

Abstract in Dutch: *In dit artikel presenteren we een nieuw type chiroptische moleculaire schakelaar waar bestraling met licht van verschillende golflengtes een reversibele helix inversie induceert van een sterisch gehinderd alkeen met een tweede chirale groep in de vorm van een stereogeen centrum aanwezig in een pyrrolidine substituent. Het extra stereogene centrum heeft een subtiele invloed op de selectiviteit tijdens het schakelen met het systeem en verbetert aanzienlijk de resolutie van de verschillende diastereomeren, wat een nadeel was van eerder gerapporteerde systemen. Daarbij komt dat de chirale pyrrolidine eenheid kleine energie verschillen tussen de verschillende toestanden van het schakelsysteem veroorzaakt wat resulteert in een kleine maar significante voorkeur voor een bepaalde richting in de helix inversie stappen.*

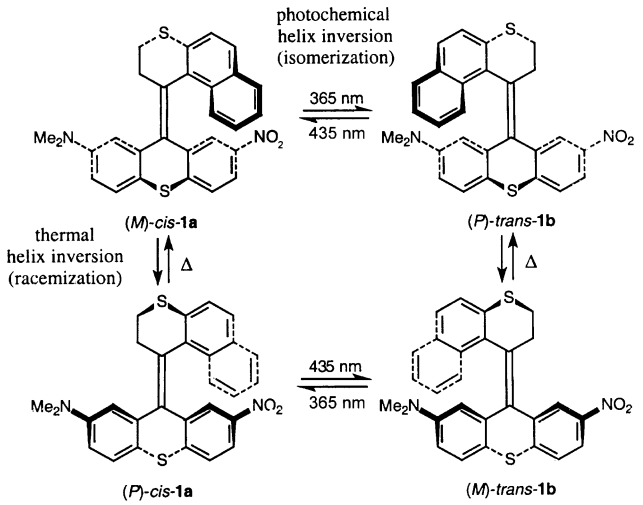

Scheme 1. Photochemical and thermal interconversion of four states of chiroptical molecular switch **1**.

ized with a dimethylamine electron donating substituent and a nitro electron withdrawing substituent. This asymmetric substitution pattern results in relatively large differences in the UV absorption characteristics of the two pseudoenantiomers that can be employed for switching. For **1**, switching between photostationary states composed of 90% (*M*)-*cis*-**1a** and 10% (*P*)-*trans*-**1b** using 435 nm light and 30% (*M*)-*cis*-**1a** and 70% (*P*)-*trans*-**1b** using 365 nm light is achieved and the switching process is reversible and repeatedly possible in *n*-hexane solution. The same holds of course for the enantiomeric couple (*P*)-*cis*-**1a** and (*M*)-*trans*-**1b** (Scheme 1 bottom). With compound **1**, clear switching between pseudoenantiomers is observed and in this way it is shown that molecular chirality can be controlled by changing only the wavelength of light used. This system has also been employed as a chiral molecular trigger in liquid crystalline systems.[21] Heating the system causes a thermal helix inversion to take place and eventually leads to racemization of both pseudoenantiomers.

The target molecule for the present study is the sterically overcrowded alkene **2**, which closely resembles donor–acceptor substituted switch **1**. The key difference in this new molecular switch is that an additional chiral unit is present. Again, the intrinsically chiral overcrowded alkene is functionalized with an electron withdrawing nitro and an electron donating amine substituent. The amine in this case is the proline-derived (*S*)-2-(methoxymethyl)pyrrolidine. This amine has been used frequently as a chiral auxiliary in asymmetric synthesis.[22] The additional stereogenic center in this molecular switch, with fixed configuration, results in four distinct diastereomeric forms, as depicted in Scheme 2, rather than two diastereomeric pairs of enantiomers as found for **1**. As a result the two photoequilibria (path a, a′) are now different and also the helix inversion steps (path b, b′) are no longer racemizations. A mutual difference in energy for the two separate *cis* ((*S*)-(*M*)-*cis*-**2a**/(*S*)-(*P*)-*cis*-**2a**) and *trans* ((*S*)-(*M*)-*trans*-**2b**/(*S*)-(*P*)-*trans*-**2b**) isomers of **2** can be anticipated.

Compound **2** offers some additional appealing features. The (*S*)-2-(methoxymethyl)pyrrolidine moiety after deprotection

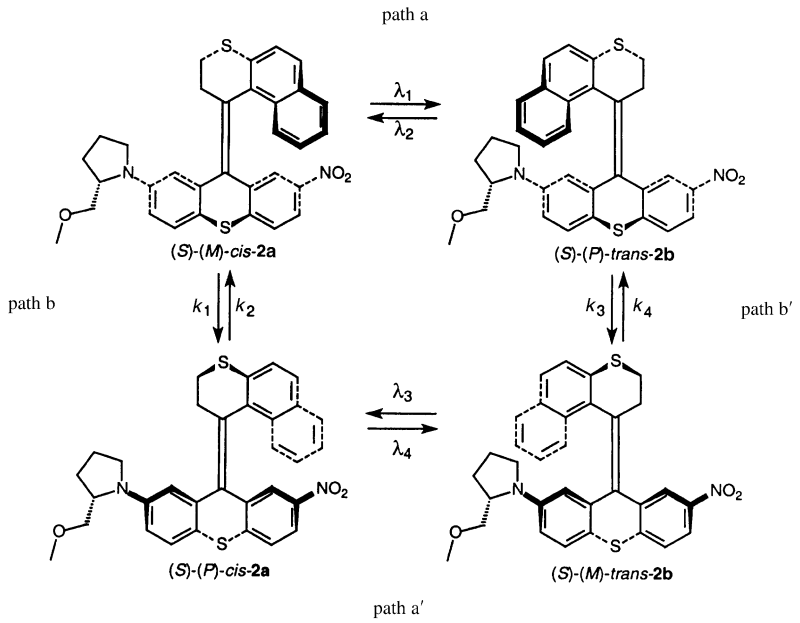

Scheme 2. Four diastereoisomers of chiroptical switch **2** and their photochemical (path a, a′) and thermal interconversions (path b, b′).

of the ether moiety might be suitable for attachment of the chiroptical switch to, for example, peptide chains, which offers an attractive route towards switchable biomaterials.[23] Another feature is that due to the diastereomeric relationship of all four forms of molecular switch **2** chiral separation techniques are no longer essential, whereas the resolution of the four stereoisomers usually is the most delicate step in our approaches towards chiroptical molecular switches and molecular motors.

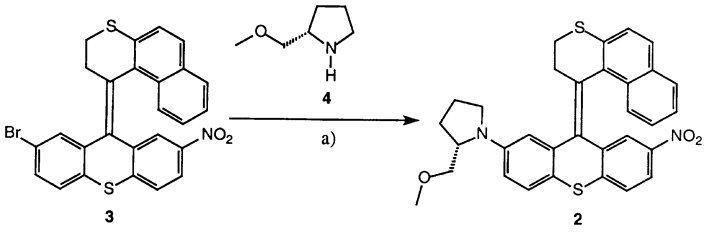

Scheme 3. Functionalization of bromo-substituted overcrowded alkene **3** to form **2** involving a palladium catalyzed amination: $[Pd_2(dba)_3]$, BINAP, NaO*t*Bu, toluene, 80 °C, yield: 58 %.

Results and Discussion

Synthesis and resolution: Compound **1** was synthesized via a linear synthesis route starting from (*N*,*N*)-dimethylaniline.[20a] Due to high stereoselectivity in the photochemical switching process of this donor–acceptor substituted compound direct access to a variety of donor–acceptor substituted chiral switches, including target compound **2**, to be able to fine tune the switching properties would be highly desirable. Therefore we altered our synthetic strategy and rather than starting from pyrrolidine functionalized starting material in a similar linear approach as for **1** a more flexible and convergent synthetic route was developed for switch **2**. This route is based on a palladium-catalyzed amination of bromo-substituted switch **3** with an appropriate amine; in the present case (*S*)-2-(methoxymethyl)pyrrolidine **4** (Scheme 3). The palladium-catalyzed amination of aryl halides has been extensively studied in recent years and numerous examples of successful arene substitutions using different amines, aryl halides and palladium catalysts have been reported.[24] We applied the Buchwald procedure in the catalytic amination shown in Scheme 3.[25]

The (*S*)-2-methoxymethylpyrrolidine was synthesized according to a literature procedure[22] starting from enantiomerically pure (*S*)-proline providing (*S*)-**4** with full retention of configuration. The bromo-substituted alkene **3** was synthesized following a route analogous to that employed for **1**. A diazo-thioketone coupling to form the central double bond, which involves the corresponding episulfide **9**, is the key step. Starting from commercially available 2-bromothiophenol and 2-chloro-5-nitrobenzoic acid the lower half thioketone **7** was obtained in three steps (Scheme 4). This thioketone was coupled with the upper half hydrazone, synthesized in three steps starting from 2-thionaphthol,[20a] via the Barton–Kellogg method.[26] Using this coupling procedure for upper and lower half, the central—sterically hindered—double bond is formed via a

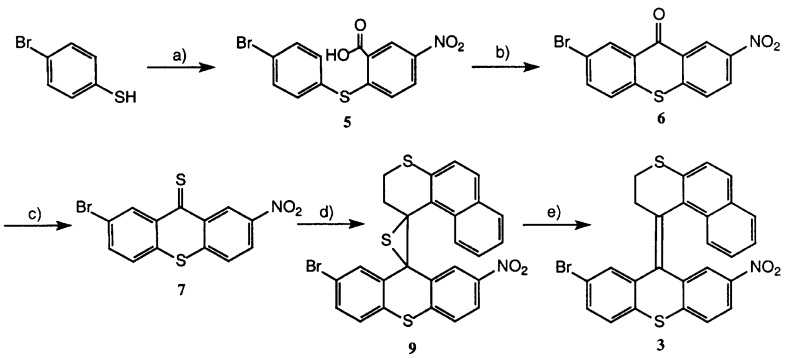

Scheme 4. Synthesis of bromo-substituted precursor **3**: a) 2-chloro-5-nitro benzoic acid, $NaHCO_3$, EtOH, Δ; b) sulfuric acid, 100 °C, 95 %; c) P_2S_5, toluene, Δ, 76 %; d) Ag_2O, $MgSO_4$, KOH/MeOH, CH_2Cl_2, $-10 \rightarrow 0$ °C, 60 %; e) Ph_3P, toluene, Δ, 97 %.

stepwise increase of the steric constraints. First, 1,3-dipolar cycloaddition of the thioketone lower half and diazo-upper half results in the formation of a five-membered thiadiazoline intermediate. Second, nitrogen is eliminated to form a three-membered episulfide. After extrusion of sulfur the desired sterically hindered alkene **3** is obtained.

Chiroptical switch **2** was obtained as a mixture of the four diastereoisomers, as depicted in Scheme 2. Separation of diastereoisomers was performed by HPLC using an achiral silica column. Employing a gradient of *n*-heptane and dichloromethane as an eluent, the four diastereomers were readily separated with retention times of 16.9 min ((*S*)-(*M*)-*cis*-**2a**), 17.4 min ((*S*)-(*P*)-*cis*-**2a**), 18.2 min ((*S*)-(*P*)-*trans*-**2b**), and 18.8 min ((*S*)-(*M*)-*trans*-**2b**). The respective (*P*)- and (*M*)-isomers could be assigned by CD spectroscopy (see below for data) and comparison with previously reported sterically overcrowded alkenes. The *cis*- and *trans*-isomers could readily be distinguished by ^{1}H NMR spectroscopy and most indicative are: i) the MeO protons which are partly shielded by the upper arene part of the molecule for the *trans*-isomers (δ 3.17 and 3.21) but not for the *cis*-isomers (δ 3.34 and 3.38) and ii) the aromatic protons of the amine-substituted arene part of the lower half which in case of the *trans*-isomer, where this part of the molecule is shielded by the upper arene part, result in distinct aromatic ^{1}H NMR signals below δ 6.50 (see Experimental Section for full NMR data).

It should be emphasized that for the chiroptical switches developed thus far, time-consuming and expensive chiral resolution was necessary, whereas in the present case achiral chromatography readily allows separation of the four stereoisomers. The accessibility of the enantiomerically pure forms is an important advantage of compound **2** over all the other chiroptical switches reported so far.[14]

Switching selectivity: Due to presence of four diastereomers, the discussion on the switching selectivity of compound **2** is a little more complicated than for our previously reported chiroptical molecular switches. Since the two photoisomerization processes in the present case are no longer enantiomeric pathways (Scheme 2), they have to be analyzed separately. For the pseudoenantiomeric couple (*S*)-(*M*)-*cis*-**2a** and (*S*)-(*P*)-*trans*-**2b** (Scheme 5), UV/Vis and CD absorption spectra were determined (Figure 2).

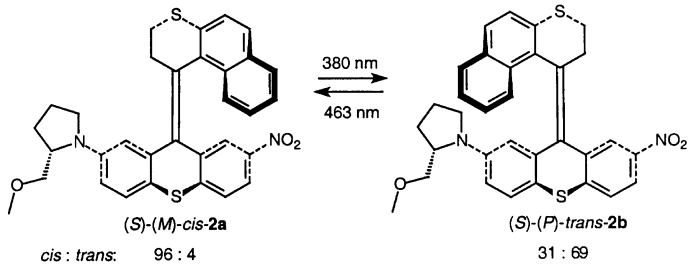

Scheme 5. Selective switching between two diastereoisomers (*S*)-(*M*)-*cis*-**2a** and (*S*)-(*P*)-*trans*-**2b**.

From the differences in the UV/Vis spectra (Figure 2a) between (*S*)-(*M*)-*cis*-**2a** (UV (*n*-hexane): λ_{max} (ε) = 255 (18610), 273 (16686), 368 (3385)) and (*S*)-(*P*)-*trans*-**2b** (UV (*n*-hexane): λ_{max} (ε) = 255 (17065), 275 (14981), 312 (6287), 327 (3882), 362 (1618), 402 (1681), with values comparable to those of other donor–acceptor switches,[20a] the ideal wavelengths for switching could be determined. The ideal wavelengths for switching are those where the ratio of the extinction coefficients of *cis*-**2a** and *trans*-**2b** show maxima and minima. Analysis of the UV spectra shows that 380 and 463 nm are the wavelengths where the highest selectivity can be expected. The CD absorption curves confirm the respective (*P*)- and (*M*)-helicity for (*S*)-(*M*)-*cis*-**2a** (CD (*n*-hexane): λ_{max} ($\Delta\varepsilon$) = 241 (−18.6), 256 (+22.6), 280 (−36.7), 326 (−1.6), 362 (+6.3)) and (*S*)-(*P*)-*trans*-**2b** (CD (*n*-hexane): λ_{max} ($\Delta\varepsilon$) = 242 (+4.4), 255 (−30.3), 275 (+28.9), 325 (+5.7), 354 (−3.9)) with $\Delta\varepsilon$ values comparable to those of the other donor–acceptor switches (e.g. compound **1**[20a]). The additional stereogenic center in the (*S*)-2-(methoxymethyl)pyrrolidine moiety has only a minor effect on the CD spectra, which are mainly determined by the exciton coupling of the upper and lower half chromophores. The CD spectra of the enantiomerically pure forms as well as the photostationary states (see below) are depicted in Figure 2b. Irradiation of an *n*-hexane solution of (*S*)-(*M*)-*cis*-**2a** with 380 nm light resulted in a photostationary state consisting of (*S*)-(*P*)-*trans*-**2b** and (*S*)-(*M*)-*cis*-**2a**

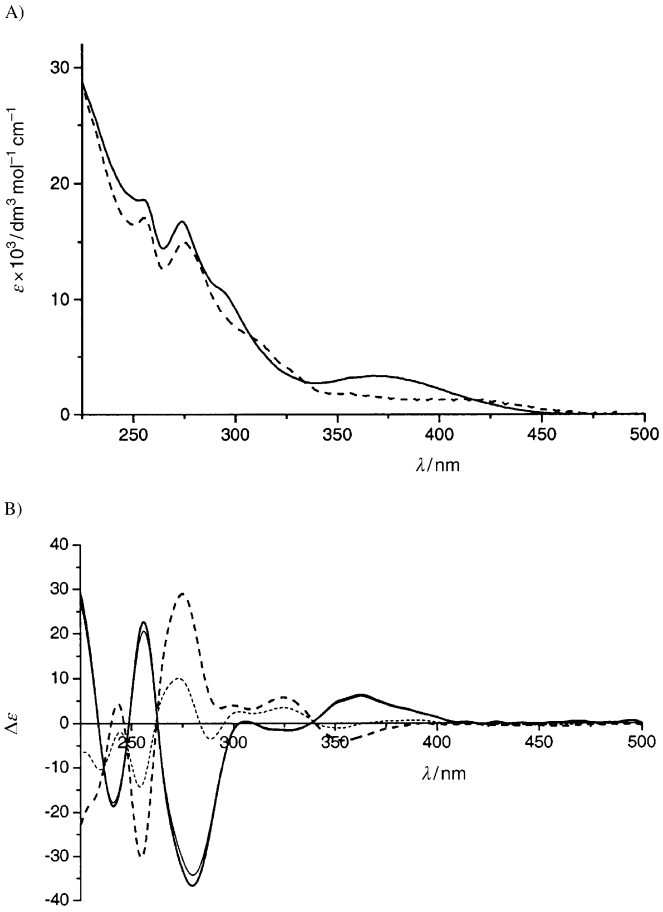

Figure 2. UV/Vis and CD absorption spectra of the diastereoisomers (*S*)-(*M*)-*cis*-**2a** and (*S*)-(*P*)-*trans*-**2b** in *n*-hexane. The solid curves correspond to (*S*)-(*M*)-*cis*-**2b** and the dashed graphs to (*S*)-(*P*)-*trans*-**2b**. The thin curves correspond to the photostationary states (solid thin: 463 nm PSS; dashed thin: 380 nm PSS).

in a ratio of 69:31, as determined by CD spectroscopy. Subsequent irradiation at 463 nm led to a photostationary state with excess (*S*)-(*M*)-*cis*-**2a**. An extremely high diastereomeric ratio (*S*)-(*M*)-*cis*-**2a**: (*S*)-(*P*)-*trans*-**2b** of 96:4 was found (see Figure 2b). The photochemical switching process is comparable to that of other donor–acceptor systems and was found to be fully reversible. The basic features of the chiroptical switching process are therefore retained despite the presence of the additional chiral auxiliary and much to our delight the stereoselectivity is improved compared with the selectivity observed for the parent compound **1**.

In a completely analogous way, the UV/Vis and CD spectra of the other pseudoenantiomeric couple (*S*)-(*P*)-*cis*-**2a** (UV (*n*-hexane): λ_{max} (ε) = 257 (23552), 287 (13652), 369 (3058); CD (*n*-hexane): λ_{max} ($\Delta\varepsilon$) = 241 (+20.7), 255 (−24.2), 280 (−37.7), 326 (+1.8), 358 (−6.5)) and (*S*)-(*M*)-*trans*-**2b** (UV (*n*-hexane): λ_{max} (ε) = 257 (20005), 271 (14895), 312 (5942), 355 (2229), 398 (1681); CD (*n*-hexane): λ_{max} ($\Delta\varepsilon$) = 243 (0), 255 (+37.7), 275 (−37.4), 325 (−7.3), 353 (+3.8)) were determined (Scheme 6 and Figure 3). The most efficient

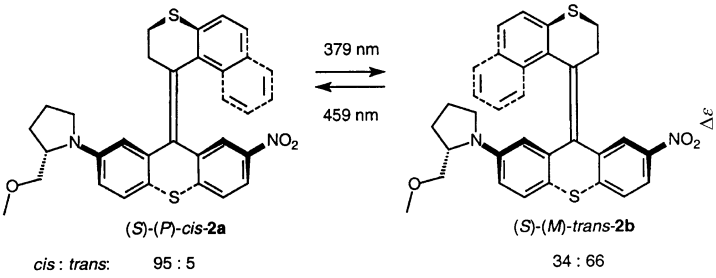

Scheme 6. Selective switching between two diastereoisomers (*S*)-(*P*)-*cis*-**2a** and (*S*)-(*M*)-*trans*-**2b**.

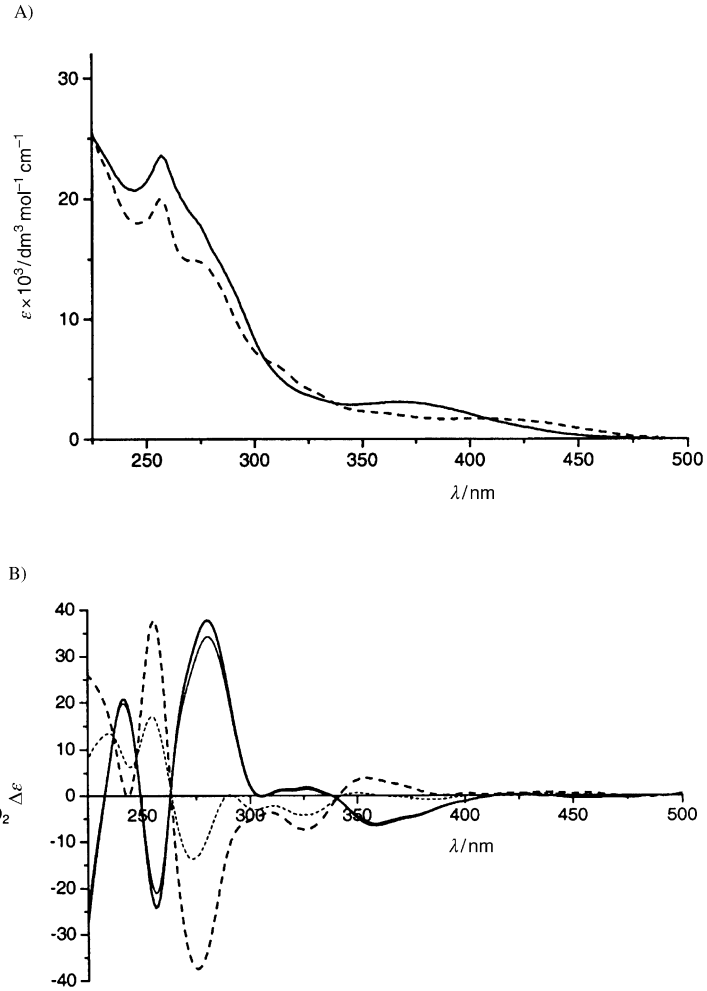

Figure 3. UV/Vis and CD absorption characteristics of the (*S*)-(*P*)-*cis*-**2a** and (*S*)-(*M*)-*trans*-**2b** diastereoisomers in *n*-hexane. The solid curves correspond to (*S*)-(*P*)-*cis*-**2a** and the dashed graphs to (*S*)-(*M*)-*trans*-**2b**. The thin curves correspond to the photostationary states (solid: 459 nm PSS; dashed: 379 nm PSS).

switching wavelengths here, again derived from the ratio of the two UV/Vis absorption curves (Figure 3a), are 379 and 459 nm for the *trans* and the *cis* photostationary state, respectively. Irradiation at 379 nm resulted in a *trans*-enriched photostationary state consisting of (*S*)-(*M*)-*trans*-**2b** and (*S*)-(*P*)-*cis*-**2a** in a 66:34 ratio. Irradiation at 459 nm resulted in the formation of a *cis*-enriched photostationary state with a ratio of (*S*)-(*P*)-*cis*-**2a**:(*S*)-(*M*)-*trans*-**2b** of 95:5. Hence, UV/Vis and CD absorption characteristics (Figure 3b) as well as switching behavior are similar for the two diastereomeric pairs of chiral photobistable molecules. This underlines the minor influence of the (*S*)-2-(methoxymethyl)pyrrolidine stereocenter on the photophysical properties. The stereoselectivity towards *trans*-**2b** in the PSS (379 nm) is, however, slightly lower for (*S*)-(*M*)-*trans*-**2b** compared with (*S*)-(*P*)-*trans*-**2b**. This is further illustrated in Figure 4 where both the UV/Vis as well as the CD absorption spectra of the respective *cis*- and *trans*-isomers are directly compared.

Subtle differences in UV absorption of the respective two *cis*- and *trans*-isomers of **2** (Figures 3 and 4 top) result in the slightly different ideal switching wavelengths (380 and 463 nm for the (*S*)-(*M*)-*cis*-**2a**/(*S*)-(*P*)-*trans*-**2b** couple versus 379 and 459 nm for the (*S*)-(*P*)-*cis*-**2a**/(*S*)-(*M*)-*trans*-**2b** couple) as well as the slightly different switching selectivity (92 and 38% versus 90 and 32% diastereomeric excess, respectively). Only small differences in CD absorptions can be observed. The CD spectra of the *cis*- and *trans*-compounds of opposite helicity are, however, still roughly mirror images. The major differences are found in the UV absorption of the two isomers at lower wavelengths with extinction coefficients $\varepsilon(\lambda)$ for (*S*)-(*M*)-*cis*-**2a** and (*S*)-(*P*)-*cis*-**2a** of 18610 (255) and 23552 (257), respectively and for (*S*)-(*P*)-*trans*-**2b** and (*S*)-(*M*)-*trans*-**2b** of 17065 (255) and 20005 (257). These differences might be assigned to different geometries of the chiral amine-substituted aryl moiety absorbing in this region but these effect were not investigated further.

Thermal stability of the distinct diastereoisomers: A small but significant effect of the additional stereogenic center in compound **2** was observed in the photophysical behavior of the four distinct diastereomers. Another important effect here is the influence of the additional stereogenic center on the thermal stability of the different stereoisomers. Where in the case of the donor–acceptor systems, thermal stability was determined by monitoring the racemization at elevated temperatures (Scheme 1), in the present system **2** one cannot

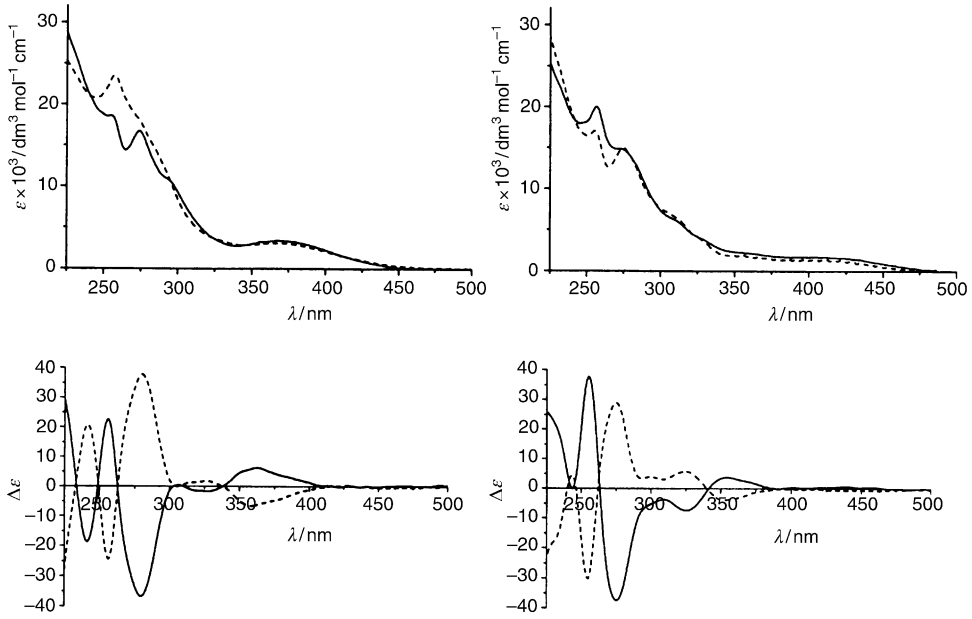

Figure 4. Comparison of UV/Vis and CD absorption characteristics of (*S*)-(*M*)-*cis*-**2a** and (*S*)-(*P*)-*cis*-**2a** (left) and (*S*)-(*M*)-*trans*-**2b** and (*S*)-(*P*)-*trans*-**2b** (right), respectively. Solid curves correspond to both the (*M*)-enantiomers; dashed curves correspond to both the (*P*)-enantiomers.

speak of a racemization but rather of a thermally induced helix inversion (Scheme 2). The thermally induced interconversion between the diastereoisomers (*S*)-(*M*)-*cis*-**2a** and (*S*)-(*P*)-*cis*-**2a** as well as between diastereoisomers (*S*)-(*M*)-*trans*-**2b** and (*S*)-(*P*)-*trans*-**2b** was monitored in *n*-dodecane by CD spectroscopy. These pairs of diastereoisomers that share the same (*cis* or *trans*) geometry but show opposite helicity might be called pseudoepimers.[27] Solutions of enantiomerically pure (*S*)-(*M*)-*cis*-**2a** and (*S*)-(*P*)-*trans*-**2b** at known concentrations were heated for 10 h at 100 °C. The change in CD absorption was monitored in time, as depicted in Figure 5.

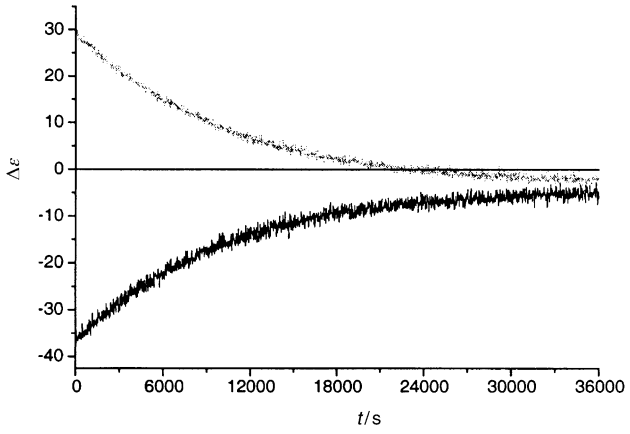

Figure 5. CD absorption (rescaled to show molar values $\Delta\varepsilon$) in time for heated samples of (*S*)-(*M*)-*cis*-**2a** (bottom) and (*S*)-(*P*)-*trans*-**2b** (top) at 100 °C in *n*-dodecane.

Knowing the molar CD absorptions of all four diastereoisomers in this solvent, which are identical to the absorptions found in *n*-hexane, the equilibrium ratio of the two respective pseudoepimers can be determined. In case of (*S*)-(*M*)-*cis*-**2a**, heating to equilibrium at 100 °C resulted in a steady state consisting of (*S*)-(*M*)-*cis*-**2a** and (*S*)-(*P*)-*cis*-**2a** in a 53.6:46.4 ratio. This steady state ratio is not 50:50 indicating that there is indeed an energy difference between the two *cis* forms of **2**. This equilibrium ratio combined with the actual rate of the pseudoracemization observed gives the rate constants of the two helix inversions: (*S*)-(*M*)-*cis*-**2a** → (*S*)-(*P*)-*cis*-**2a** (k_1) and (*S*)-(*P*)-*cis*-**2a** → (*S*)-(*M*)-*cis*-**2a** (k_2).[28] The observed pseudoracemization rate in this case is $9.9 \times 10^{-5}\ s^{-1}$ and the rate constants of the two helix inversion pathways were determined to be 4.6×10^{-5} and $5.3 \times 10^{-5}\ s^{-1}$, respectively, for k_1 and k_2 (Scheme 7). In case of the (*S*)-(*P*)-*trans*-**2b** solution at 100 °C, an equilibrium state of (*S*)-(*P*)-*trans*-**2b** and (*S*)-(*M*)-*trans*-**2b** in a ratio of 47.5:52.5 was obtained. Also for the two *trans* forms of **2**, the anticipated energy difference is observed. Again, combining the equilibrium ratio with the actual rate of the pseudoracemization process (in this case $9.5 \times 10^{-5}\ s^{-1}$) gives the rate constants of the two helix inversions. The rate constants for the two processes (*S*)-(*P*)-*trans*-**2b** (*S*)-(*M*)-*trans*-**2b** (k_3) and (*S*)-(*M*)-*trans*-**2b** (*S*)-(*P*)-*trans*-**2b** (k_4) were determined to be 5.0×10^{-5} and $4.5 \times 10^{-5}\ s^{-1}$, respectively. From these k values, the Gibbs energy of activation of the four distinct thermal pathways, which is an indication for the relative stability of the four isomers, can be determined.[28] The calculated values are depicted in Scheme 7 and these values again show a small but significant difference for the forward and backward helix inversion for both *cis*-**2a** and *trans*-**2b**. Although the additional stereogenic center clearly has an effect on the relative stability of the distinct isomers the effects are rather small. It should be noted that both for the *trans* as well as the *cis*-isomers (*M*)-helicity is preferred, however, no explanation for this behavior can be given at this moment.

It might seem unexpected that the energy difference between the two *trans*-nitro isomers is in fact smaller than the difference for the two *cis*-nitro isomers. At first inspection of the molecular structures it would seem that the influence of the stereogenic center of the pyrrolidine substituent, which is solely responsible for the observed energy differences between the *cis*-isomers (and the *trans*-isomers), is larger when the pyrrolidine moiety is in close proximity to the sterically demanding upper arene part of the molecule. It was, however, previously observed that in these complicated helical structures the methylene group directly adjacent to the central double bond in the upper half of the molecule has a

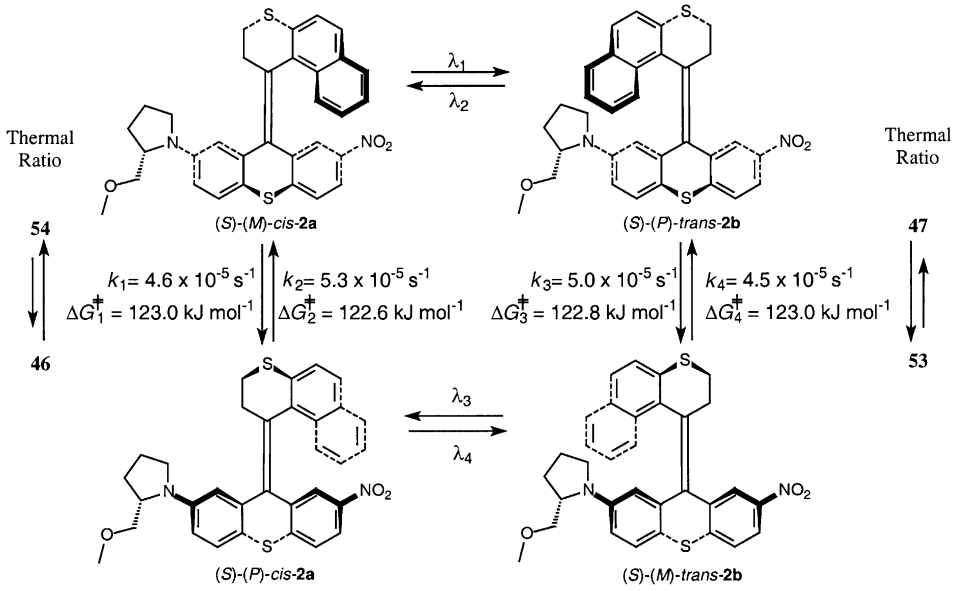

Scheme 7. Thermal stabilities for the four distinct diastereoisomers of **2**.

substantial steric effect on the lower half.[29] Whereas the two hydrogens are restricted to their respective axial and equatorial orientation, the naphthalene moiety in the *trans*-isomer can simply bend away thereby greatly reducing the steric effect exerted on the lower half of the molecule. Therefore a distinct difference exists between *trans*- and *cis*-isomers, where the pyrrolidine-moiety is facing a naphthalene or CH_2 group in the upper half, respectively.

Conclusion

We presented a novel donor–acceptor substituted molecular switch **2** with excellent switching properties. A new and more efficient synthetic route towards these systems was developed which opens up the possibility of synthesizing a variety of donor–acceptor systems in one step starting from a mutual bromo-substituted synthon **3**. Compound **2** has some advantageous properties compared with previously reported donor–acceptor switches. The improved resolution properties of the system in combination with a high switching selectivity make this compound a useful member of the chiroptical molecular switch family. The additional stereogenic center only has a minor effect on the photophysical properties and the thermal stabilities of the different stereoisomers. Nevertheless, for a comparable class of sterically overcrowded alkene the presence of a single stereogenic center, in addition to the intrinsic chirality of the system, resulted in completely controlled unidirectional rotation in two generations of molecular motors. The key feature in these systems is unidirectionality in the thermal helix inversion steps as a result of a relatively large energy differences between the two pseudoenantiomeric forms. Although the energy differences for compound **2**, shown in Scheme 7, are too small for a full control over the directionality in these isomerization processes, the influence of the additional stereogenic center in this molecule can be compared to the influence of the stereogenic center in the molecular motor systems, albeit far less pronounced. The delicate balance of chiral influences on these intrinsically chiral helically shaped overcrowded systems and the stereochemical parameters controlling the thermal and photochemical processes remains an interesting topic for further studies.

Experimental Section

General methods: ^{1}H NMR spectra were recorded on a Varian Gemini-200 (200 MHz), a Varian VXR-300 (300 MHz) or a Varian Unity Plus Varian-500 (500 MHz). ^{13}C NMR spectra were recorded on a Varian Gemini-200 (50 MHz), a Varian VXR-300 (75 MHz) or a Varian Unity Plus Varian-500 (125 MHz). Chemical shifts are denoted in δ-unit (ppm) relative to $CDCl_3$. The splitting patterns are designated as follows: s (singlet), d (doublet), t (triplet), q (quartet), m (multiplet) and br (broad) for ^{1}H NMR. For ^{13}C NMR the carbon atoms are assigned as q (primary carbon), t (secondary carbon), d (tertiary carbon) and s (quaternary carbon). CD spectra were recorded on a JASCO J-715 spectropolarimeter and UV measurements were performed on a Hewlett-Packard HP 8453 FT Spectrophotometer using UVASOL grade solvents (Merck). MS spectra were obtained with a Jeol JMS-600 spectrometer by Mr. A.Kieviet. Column chromatography was performed on silica gel (Aldrich 60, 230–400 mesh). HPLC analyses were performed on a Waters HPLC system equipped with a 600E solvent delivery system and a 996 Photodiode Array Detector. Preparative HPLC was performed by Mr. M. B. van Gelder on a preparative Gilson HPLC system consisting of a 231XL sampling injector, a 306 (10SC) pump, an 811C dynamic mixer, a 805 manometric module, with a 119 UV/Vis detector and a 202 fraction collector, using the (chiral) columns as mentioned. Elution speed was 1 mL min^{-1}, unless stated otherwise. Solvents were distilled and dried before use, if necessary, by standard methods. Reagents and starting materials were used as obtained from Aldrich, Acros, Fluka or Merck. (*S*)-proline obtained from Acros and reported 99+ % was used as purchased.

Irradiation experiments: Irradiations were performed with an 150 W Oriel Xe lamp attached to an Oriel monochromator or a 180 W Oriel Hg lamp adapted with a suitable Mercury line filter for 313, 365, 405 and 435 nm irradiations (typical bandwidth 10 nm). Photostationary states are ensured by monitoring composition changes in time by taking UV spectra at distinct intervals until no changes were observed. Ratios of the different forms of the molecular switches were determined by HPLC by monitoring at the isosbestic point or by NMR analysis. HPLC elution times and NMR details are denoted throughout the synthetic procedures. CD spectra were recorded on a JASCO J-715 spectropolarimeter and UV measurements were performed with a Hewlett–Packard HP 8453 FT spectrophotometer using UVASOL grade solvents (Merck). Thermal helix inversions were also monitored by CD spectroscopy employing a JASCO PFD-350S/350L Peltier type FDCD attachment with temperature control.

2,3-Dihydro-1*H*-naphtho[2,1-b]thiopyran-1-one hydrazone (8):[20a] 2,3-Dihydro-1*H*-naphtho[2,1-b]thiopyran-1-one hydrazone was synthesized as described before starting from 2-thionaphthol, via 3-(2-naphthylthio)-propiononitrile and 2,3-dihydro-1*H*-naphtho[2,1-b]thiopyran-1-one. ^{1}H NMR: $\delta = 2.87$ (s, 4H), 5.43 (brs, 2H), 7.31 (d, $J = 8.4$ Hz, 1H), 7.37 (ddd, $J = 8.1, 7.0, 1.1$ Hz, 1H), 7.46 (ddd, $J = 8.8, 7.0, 1.5$ Hz, 1H), 7.58 (d, $J = 8.4$ Hz, 1H), 7.72 (dd, $J = 8.1, 1.5$ Hz, 1H), 8.65 (d, $J = 8.8$ Hz, 1H); ^{13}C NMR $\delta = 27.27$ (t), 30.31 (t), 124.93 (d), 126.37 (d), 126.46 (d), 126.66 (d), 127.59 (d), 127.85 (d), 129.60 (s), 131.39 (s), 132.94 (s), 135.94 (s), 145.23 (s).

(*S*)-2-(Methoxymethyl)pyrrolidine (4):[22] Under exclusion of oxygen, $LiAlH_4$ (14 g, 0.4 mol) and anhydrous THF (600 mL) were heated under reflux for 15 min. Without heating, (*S*)-proline (25 g, 0.25 mol) was added in small portions and the mixture was subsequently heated for 1 h under reflux. Excess $LiAlH_4$ was decomposed by cautiously adding a solution of KOH (7 g) in H_2O (28 mL). After stirring for 15 min the mixture was filtered and the remaining salts were extracted with THF (200 mL). The combined organic filtrates were dried (Na_2SO_4) and concentrated under reduced pressure at 30 °C. Methyl formate (18 mL, 17 g, 0.28 mol) was added at 0 °C over a period of 1 h to the crude product and the mixture was stirred for 2 h. Excess methyl formate was evaporated at 30 °C in vacuo affording a dark oil which was taken up in CH_2Cl_2 (150 mL) and dried with Na_2SO_4. The mixture was filtered and concentrated under reduced pressure at 30 °C. The procedure yielded the crude N-formyl compound (28.3 g, ca. 0.22 mol), which was dissolved in anhydrous THF (350 mL). The solution was cooled to −60 °C and MeI (18 mL, 0.26 mol) and NaH (6.26 g, 0.26 mol) were added carefully. The solution was allowed to warm to RT (H_2 gas evolves), heated under reflux for 15 min, quenched by slow addition of 6 M HCl (20 mL) and filtered. THF was evaporated under reduced pressure yielding a dark oil. A solution of KOH (40 g) in H_2O (156 mL) was added to the crude product under vigorous stirring at RT and the mixture was heated under reflux for 5 h. (*S*)-2-(Methoxymethyl)pyrrolidine was extracted in a 500 mL perforator over a period of 24 h with diethyl ether. The organic layer was dried using Na_2SO_4, diethyl ether was evaporated and product purified using bulb-to-bulb distillation (b.p. 62 °C at 40 Torr). The procedure yielded **4** as a colorless liquid (10.56 g, 37% overall yield) which was stored at −4 °C. Optical rotation was in accordance with literature.[30] ^{1}H NMR: $\delta = 1.23-1.30$ (m, 1H), 1.56–1.72 (m, 3H), 2.44 (s, 1H), 2.71–2.87 (m, 2H), 3.11–3.21 (s, 3H); ^{13}C NMR: $\delta = 23.72$ (t), 26.27 (t), 44.82 (t), 56.11 (q), 57.36 (d), 74.58 (t).

2-[(4-Bromophenyl)sulfanyl]-5-nitrobenzoic acid (5): *p*-Bromothiophenol (12 g, 64 mmol) and 2-chloro-5-nitrobenzoic acid (13.14 g, 64 mmol) were added to a solution of $NaHCO_3$ (10.8 g, 128 mmol) in dry ethanol (200 mL). The reaction mixture was heated under reflux for 24 h under a nitrogen atmosphere. After this period a 10% aq. HCl solution (150 mL) was added, after which a precipitate was collected by filtration, yielding crude **5** (22.1 g, 98%) as a yellow solid, which was used without further purification.

2-Bromo-7-nitro-9*H*-thioxanthen-9-one (6): A suspension of **5** (22.1 g, 62 mmol) in sulfuric acid (400 mL) was stirred and heated at 100 °C for 3 h. The suspension was then poured onto ice (500 g) and left overnight. Next the precipitate was filtered and washed with water (2 × 50 mL), concentrated $NaHCO_3$ (2 × 100 mL) and ethanol (2 × 50 mL). The yellow solid was dried at 60 °C under reduced pressure, yielding **6** (20.2 g, 97%). m.p. 288.1–290.5 °C; ^{1}H NMR: $\delta = 7.46$ (d, $J = 8.4$ Hz, 1H), 7.70 (d, $J = 8.8$ Hz, 1H), 7.76 (dd, $J = 8.4$, 2.2 Hz, 1H), 8.39 (dd, $J = 9.2$, 2.6 Hz, 1H), 8.72 (d, $J = 2.2$ Hz, 1H), 9.38 (d, $J = 2.2$ Hz, 1H); no ^{13}C data available due to low solubility; HRMS: *m*/*z*: calcd for $C_{13}H_6BrNO_3S$: 334.92512; found: 334.92661.

2-Bromo-7-nitro-9*H*-thioxanthene-9-thione (7): A suspension of xanthone **6** (5.1 g, 15 mmol) and P_2S_5 (8 g, 36 mmol) in dry toluene (150 mL) was refluxed for 72 h. After this period additional P_2S_5 (3 g, 14 mmol) was added and the suspension was heated under reflux for another 3 h. The suspension was then allowed to cool to about 50 °C and filtered. The flask was washed with hot toluene until the solvent was no longer green. From the filtered solution the solvent was evaporated to leave a brown solid. Recrystallization from toluene yielded **7** as dark brown crystals (4.0 g, 76%). M.p. 274.8–276.3 °C; ^{1}H NMR: $\delta = 7.43$ (d, $J = 8.4$ Hz, 1H), 7.66 (d, $J = 8.8$ Hz, 1H), 7.73 (dd, $J = 8.4$, 2.2 Hz, 1H), 8.34 (dd, $J = 9.2$, 2.6 Hz, 1H), 9.00 (d, $J = 2.2$ Hz, 1H), 9.68 (d, $J = 2.6$ Hz, 1H); no ^{13}C data available due to low solubility; HRMS: *m*/*z*: calcd for $C_{13}H_6BrNO_2S_2$: 350.90228; found: 350.90238.

Dispiro[1,2,3,4-tetrahydrophenanthrene-4,2′-thiirane-3′,9″-7-bromo-2″-nitro))-9″*H*-thioxanthene (9): A stirred solution of hydrazone **8** (350 mg, 1.53 mmol) in dry CH_2Cl_2 (20 mL) was cooled to −20 °C, whereupon $MgSO_4$ (600 mg), Ag_2O (531 mg, 2.29 mmol) and a saturated solution of KOH in dry MeOH (1.2 mL) were successively added and the mixture was stirred at this temperature under a nitrogen atmosphere. After the solution turned deep red it was filtered into another ice-flask containing thioketone **7** (445 mg, 1.53 mmol) and the mixture was then stirred for another 3 h while warming to room temperature. The precipitated solid (excess **7**) was filtered off and the solvent was evaporated. The product was purified by column chromatography (silica gel, CH_2Cl_2/hexane 1:1), yielding **9** (510 mg, 60.1%) as a yellow powder as a 1:1 mixture of *cis*- and *trans*-isomers. HRMS: *m*/*z*: calcd for $C_{26}H_{16}BrNO_2S_3$: 550.95060; found: 550.95225.

7-Bromo-2-nitro-9-(1′,2′,3′,4′-tetrahydrophenanthrene-4′ylidene)-9*H*-thioxanthene (3): Triphenylphosphine (0.39 g, 1.5 mmol) was added to a stirred solution of episulfide **9** (0.510 g, 0.92 mmol) in toluene (50 mL) and the resulting solution was refluxed for 3 d. The solvent was evaporated and the resulting orange solid was recrystallized from 96% EtOH to yield **3** as an approximate 1:1 mixture of isomers as a yellow powder (491 mg, 97%). ^{1}H NMR: $\delta = 2.30-2.40$ (m, 3H), 3.45–3.64 (m, 8H), 6.53 (d, $J = 1.8$ Hz, 1H), 6.87–7.16 (m, 10H), 7.32–7.71 (m, 22H), 8.14 (dd, $J = 8.4$, 2.2 Hz, 1H), 8.37 (d, $J = 2.2$ Hz, 1H); HRMS: *m*/*z*: calcd for $C_{26}H_{16}BrNO_2S_2$: 518.97853; found: 518.97674; elemental analysis calcd (%) for $C_{26}H_{16}BrNO_2S_2$: C 60.24, H 3.11, N 2.70, S 12.37; found: C 60.33, H 3.05, N 2.86, S 12.69.

7-((*S*)-2-(Methoxymethyl)pyrrolidine)-2-nitro-9-(1′,2′,3′,4′-tetrahydrophenanthrene-4′ylidene)-9*H*-thioxanthene (2): BINAP (15 mg, 0.0225 mmol) and $[Pd_2(dba)_3]$ (7.5 mg, 0.0063 mmol) were dissolved in dry toluene (50 mL). This solution was stirred for 30 min at RT, whereupon it turned from dark red to dark orange. After this period NaO*t*Bu (125 mg, 1.3 mmol) was added, followed by bromo-substituted alkene **3** (100 mg, 0.19 mmol) and (*S*)-2-(methoxymethyl)pyrrolidine (**4**; 50 mg, 0.43 mmol). The mixture was stirred at 80 °C for 2 d. Subsequently the reaction mixture was poured into CH_2Cl_2 (50 mL). After filtration the solvents were evaporated. The crude product was dissolved in a small amount of CH_2Cl_2 and purified using column chromatography (silica gel; CH_2Cl_2/*n*-hexane/NEt_3 50:50:1) to afford **2** as a red solid mixture of stereoisomers (60 mg, 58%). HRMS: *m*/*z*: calcd for $C_{32}H_{28}N_2O_3S_2$: 552.15411; found: 552.15296.

Separation of stereoisomers was performed by HPLC (Econosphere Silica; 5 μm; 250 × 4.6 mm). The following gradient of *n*-heptane and dichloromethane was used as an eluent: 0–3 min pure *n*-heptane; 3–15 min gradient *n*-heptane/dichloromethane 100:0 to 0:100; 15–20 min pure dichloromethane; 20–21 min gradient *n*-heptane/dichloromethane 0:100 to 100:0. The four diastereomers are readily separated with retention times of 16.9 min ((*S*)-(*M*)-*cis*-**2a**); 17.4 min ((*S*)-(*P*)-*cis*-**2a**); 18.2 min ((*S*)-(*P*)-*trans*-**2b**); 18.8 min ((*S*)-(*M*)-*trans*-**2b**). The respective (*M*)- and (*P*)-isomers were assigned by comparison of the CD spectra with other sterically overcrowded alkenes synthesized. The respective *cis*- and *trans*-isomers were assigned by ^{1}H NMR (see below).

^{1}H NMR: (*S*)-(*M*)-*cis*-**2a** and (*S*)-(*P*)-*cis*-**2a**: $\delta = 1.92-2.06$ (m, 8H), 2.24–2.31 (m, 2H), 3.08–3.26 (m, 4H), 3.34 (s, 3H), 3.38 (s, 3H), 3.43–3.58 (m, 8H), 3.76–3.88 (m, 3H), 3.90–3.98 (m, 1H), 6.59 (t, $J = 2.2$ Hz, 1H), 6.62 (t, $J = 2.2$ Hz, 1H), 6.87 (t, $J = 2.6$ Hz, 2H), 6.91–6.96 (m, 2H), 7.01–7.06 (m, 2H), 7.18–7.24 (m, 2H), 7.28–7.59 (m, 14H); (*S*)-(*M*)-*trans*-**2b** and (*S*)-(*P*)-*trans*-**2b**: $\delta = 1.92-2.06$ (m, 8H), 2.24–2.31 (m, 2H), 3.08–3.26 (m, 4H), 3.17 (s, 3H), 3.21 (s, 3H), 3.43–3.58 (m, 8H), 3.76–3.88 (m, 3H), 3.90–3.98 (m, 1H), 5.77 (d, $J = 2.2$ Hz, 1H), 5.87 (d, $J = 2.2$ Hz, 1H), 6.08 (dd, $J = 8.4$, 2.2 Hz, 1H), 6.14 (dd, $J = 8.4$, 2.2 Hz, 1H), 7.01–7.16 (m, 6H), 7.47–7.60 (m, 8H), 7.67 (d, $J = 8.4$ Hz, 2H), 8.07–8.13 (m, 2H), 8.34 (d, $J = 2.2$ Hz, 1H), 8.39 (d, $J = 2.2$ Hz, 1H).

(*S*)-(*M*)-*cis*-**2a**: UV/Vis (*n*-hexane): λ_{max} (ε) = 255 (18610), 273 (16686), 368 (3385); CD (*n*-hexane): λ_{max} ($\Delta\varepsilon$) = 241 (−18.6), 256 (+22.6), 280 (−36.7), 326 (−1.6), 362 (+6.3).

(*S*)-(*P*)-*cis*-**2a**: UV/Vis (*n*-hexane): λ_{max} (ε) = 257 (23552), 287 (13652), 369 (3058); CD (*n*-hexane): λ_{max} ($\Delta\varepsilon$) = 241 (+20.7), 255 (−24.2), 280 (−37.7), 326 (+1.8), 358 (−6.5).

(*S*)-(*M*)-*trans*-**2b**: UV/Vis (*n*-hexane): λ_{max} (ε) = 257 (20005), 271 (14895), 312 (5942), 355 (2229), 398 (1681); CD (*n*-hexane): λ_{max} ($\Delta\varepsilon$) = 243 (0), 255 (+37.7), 275 (−37.4), 325 (−7.3), 353 (+3.8).

(*S*)-(*P*)-*trans*-**2b**: UV/Vis (*n*-hexane): λ_{max} (ε) = 255 (17065), 275 (14981), 312 (6287), 327 (3882), 362 (1618), 402 (1681); CD (*n*-hexane): λ_{max} ($\Delta\varepsilon$) = 242 (+4.4), 255 (−30.3), 275 (+28.9), 325 (+5.7), 354 (−3.9).

[1] *Sci. Amer.* Special Issue: *Nanotech: The Science of Small Gets Down to Business*, September **2001**; b) R. P. Feynman in *Miniturization* (Ed.: H. D. Gilbert), New York, **1971**; c) K. E. Drexler, *Nanosystems: Molecular Machinery, Manufacturing and Computation*, Wiley, New York, **1992**; d) R. D. Astumian, *Sci. Amer.* **2001**, *285(1)*, 56–64.

[2] T. R. Kelly, M. C. Bowyer, K. V. Bhaskar, D. Bebbington, A. Gracia, F. R. Lang, M. H. Kim, M. P. Jette, *J. Am. Chem. Soc.* **1994**, *116*, 3657–3658.

[3] a) A. M. Stevens, C. J. Richards, *Tetrahedron Lett.* **1997**, *38*, 7805–7808; b) J. Clayden, J. H. Pink, *Angew. Chem.* **1998**, *110*, 2040–2043; *Angew. Chem. Int. Ed.* **1998**, *37*, 1937–1939.

[4] T. C. Bedard, J. S. Moore, *J. Am. Chem. Soc.* **1995**, *117*, 10662–10671.

[5] M. C. Jiménez, C. Dietrich-Buchecker, J.-P. Sauvage, *Angew. Chem.* **2000**, *112*, 3422–3425; *Angew. Chem. Int. Ed.* **2000**, *39*, 3284–3287.

[6] *Molecular Switches* (Ed.: B. L. Feringa), Wiley-VCH, Weinheim, **2001**.

[7] *Special Issue*: Photochromism: Memories and Switches, *Chem. Rev.* **2000** (Guest Ed.: M. Irie), *100*, 1683–1890.

[8] See for example: a) N. P. M. Huck, W. F Jager, B. de Lange, B. L. Feringa, *Science* **1996**, *273*, 1686–1688; b) M. Suarez, G. B. Schuster, *J. Am. Chem. Soc.* **1995**, *117*, 6732–6738.

[9] See for example: a) C. Denekamp, B. L. Feringa, *Adv. Mater.* **1998**, *10*, 1080–1082; b) K. Matsuda, S. Yamamoto, M. Irie, *Tetrahedron Lett.* **2001**, *42*, 7291–7293.

[10] Most examples employ chiral azobenzene switches in liquid crystals: a) T. Ikeda, T. Sasaki, K. Ichimura, *Nature* **1993**, *361*, 428–430; b) T. Kusumoto, K. Sato, K. Ogino, T. Hiyama, S. Takehara, M. Osawa, K. Nakamura, *Mol. Cryst. Liq. Cryst.* **1993**, *14*, 727–732; c) M. Negishi, O. Tsutsumi, T. Ikeda, T. Hiyama, J. Kawamura, M. Aizawa, S. Takehara, *Chem. Lett.* **1996**, 319–320; d) M. Negishi, K. Kanie, T. Ikeda, T. Hiyama, *Chem. Lett.* **1996**, 583–584; e) T. Ikeda, O. Tsutsumi, *Science* **1995**, *268*, 1873–1875.

[11] a) L. Eggers, V. Buβ, *Angew. Chem.* **1997**, *109*, 885—887; *Angew. Chem. Int. Ed. Engl.* **1997**, *36*, 881–883; b) A. Miyashita, A. Iwamoto, T. Kuwayama, H. Shitara, Y. Aoki, M. Hirano, H. Nohira, *Chem. Lett.* **1997**, 965–966.

[12] a) Y. Yokoyama, Y. Shimizu, S. Uchida, Y. Yokoyama, *J. Chem. Soc. Chem. Commun.* **1995**, 785–786; b) Y. Yokoyama, S. Uchida, Y. Yokoyama, Y. Sugawara, Y. Kurita, *J. Am. Chem. Soc.* **1996**, *118*, 3100–3107.

[13] See for example: a) O. Pieroni, A. Fissi, G. Popova, *Prog. Polym. Sci.* **1998**, *23*, 81–123; b) F. Ciardelli, O. Pieroni, A. Fissi, C. Carlini, A. Altomare, *Br. Polym. J.* **1989**, *21*, 97–106; c) M. Irie, *Adv. Polym. Sci.* **1990**, *94*, 27–67; d) *Applied Photochromic Polymer Systems* (Ed.: C. B. McArdle), Blackie, Glasgow (UK), **1992**; e) O. Pieroni, F. Ciardelli, *Trends Polym. Sci.* **1995**, *3*, 282–287; f) T. Kinoshita, *Prog. Polym. Sci.* **1995**, *20*, 527–583; g) I. Willner, *Acc. Chem. Res.* **1997**, *30*, 347–356.

[14] a) B. L. Feringa, R. A. van Delden, N. Koumura, E. M. Geertsema, *Chem. Rev.* **2000**, *100*, 1789–1816; b) B. L. Feringa, R. A. van Delden, M. K. J. ter Wiel in *Molecular Switches* (Ed.: B. L. Feringa), Wiley-VCH, Weinheim, **2001**, Chapter 5, pp. 123–163.

[15] B. L. Feringa, N. P. M. Huck, H. A. van Doren, *J. Am. Chem. Soc.* **1995**, *117*, 9929–9930.

[16] a) N. Koumura, R. W. J. Zijlstra, R. A. van Delden, N. Harada, B. L. Feringa, *Nature* **1999**, *401*, 152–155; b) B. L. Feringa, N. Koumura, R. A. van Delden, M. K. J. ter Wiel, *Appl. Phys. A* **2002**, *75*, 301–308; c) B. L. Feringa, *Acc. Chem. Res.* **2001**, *34*, 504–513.

[17] R. A. van Delden, N. Koumura, N. Harada, B. L. Feringa, *Proc. Nat. Acad. Sci.* **2002**, *99*, 4945–4949.

[18] a) N. Koumura, E. M. Geertsema, A. Meetsma, B. L. Feringa, *J. Am. Chem. Soc.* **2000**, *122*, 12005–12006; b) N. Koumura, E. M. Geertsema, M. B. van Gelder, A. Meetsma, B. L. Feringa, *J. Am. Chem. Soc.* **2002**, *124*, 5037–5051.

[19] For stereochemical definitions see: E. L. Eliel, S. H. Wilen, *Stereochemistry of Organic Compounds*, Wiley, New York, **1994**.

[20] a) W. F. Jager, J. C. de Jong, B. de Lange, N. P. M. Huck, A. Meetsma, B. L. Feringa, *Angew. Chem.* **1995**, *107*, 346–349; *Angew. Chem. Int. Ed. Engl.* **1995**, *34*, 348–350; b) N. P. M. Huck, B. L. Feringa, *J. Chem. Soc. Chem. Commun.* **1995**, 1095–1096.

[21] B. L. Feringa, N. P. M. Huck, H. A. van Doren, *J. Am. Chem. Soc.* **1995**, *117*, 9929–9930.

[22] D. Enders, M. Klatt, *Synthesis* **1996**, 1403–1421.

[23] For an account on biomolecular switches, see: I. Willner, B. Willner in *Molecular Switches* (Ed.: B. L. Feringa), Wiley-VCH, Weinheim, **2001**, Chapter 6, pp. 165–218.

[24] See for example: a) J. P. Wolfe, S. Wagaw, J.-F. Marcoux, S. L. Buchwald, *Acc. Chem. Res.* **1998**, *31*, 805–818; b) B. H. Yang, S. L. Buchwald, *J. Organomet. Chem.* **1999**, *576*, 125–146; c) A. R. Muci, S. L. Buchwald, *Top. Curr. Chem.* **2002**, *219*, 131–209.

[25] J. P. Wolfe, S. L. Buchwald, *J. Org. Chem.* **2000**, *65*, 1144–1157.

[26] a) D. H. R. Barton, B. J. Willis, *J. Chem. Soc. Chem. Commun.* **1970**, 1225–1226; b) R. M. Kellogg, J. Buter, S. Wassenaar, *J. Org. Chem.* **1972**, *37*, 4045–4060.

[27] Based on the term pseudoenantiomers; for stereochemical definitions see ref. [19].

[28] The measured rate constant k for the process is a sum of the two individual rate constants of the reversible helix inversion, for *cis*-**2a**: (*M*)-*cis*-**2a** (*P*)-*cis*-**2a** rate: k_1; (*P*)-*cis*-**2a** (*M*)-*cis*-**2a** rate: k_2 then $k_{measured} = k_1 + k_2$. The ratio of the two components at equilibrium [(*M*)-*cis*-**2a**]/[(*P*)-*cis*-**2a**] $= K = k_2/k_1$ was determined separately resulting in two equations with two unknown parameters that can be solved. For a unimolecular reaction $\Delta G^{+} = -RT\ln(kh/k_bT)$.

[29] A. M. Schoevaars, W. Kruizinga, R. W. J. Zijlstra, N. Veldman, A. L. Spek, B. L. Feringa, *J. Org. Chem.* **1997**, *62*, 4943–4948.

[30] D. Seebach, H.-O. Kalinowski, B. Bastini, G. Crass, H. Daum, H. Dörr, N. P. DuPreez, V. Ehrig, W. Langer, C. Nüssler, H.-A. Oei, M. Schmidt, *Helv. Chim. Acta* **1977**, *60*, 301–325.

Received: December 12, 2002 [F4660]

